Inorganic Chemistry

Article

pubs.acs.org/IC

Anion-Exchange-Driven Disassembly of a SiO_2/CTAB Composite Mesophase: the Formation of Hollow Mesoporous Silica Spheres

Qiyu Yu, Junfeng Hui, Pengpeng Wang, and Xun Wang*

Department of Chemistry, Tsinghua University, Beijing 100084, People's Republic of China

Supporting Information

ABSTRACT: Silica-based surfactant/inorganic composite mesophases have been extremely studied. In this work, we developed a mild method to realize the room-temperature disassembly of a SiO_2/cetyltrimethylammonium bromide (CTAB) mesophase in a neutral medium. Using $KMnO_4$ as a typical etching agent, SiO_2/CTAB mesophase spheres were partially disassembled into normal or rattle-type hollow structures. The disassembly of the SiO_2/CTAB spheres was supposed to be driven by anion exchange between permanganate and silicate ions. This unique method makes possible the selective etching of a SiO_2/CTAB mesophase over a SiO_2 phase.

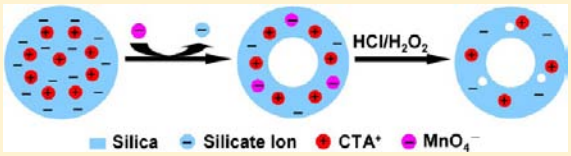

INTRODUCTION

Surfactant/inorganic (SI) composite mesophases have been extensively studied because of their wide application in the fabrication of advanced materials and their fundamental significance in chemical aspects of biomineralization. The inorganic moiety of the hybrid materials can be silicate, metal oxide, polyoxometalate, metal halide, and so on.[1−6] The surfactant and the inorganic moieties are coassembled via relatively weak noncovalent interactions. Therefore, these mesophase materials, under certain conditions, may be structurally rearranged or disassembled, which is important to the fabrication of new functional materials.[4b,7−9] However, related studies mainly focus on the bottom-up fabrication of various mesophase SI composite materials; the rearrangement or disassembly of preformed SI composites is relatively less studied.

Silica-based SI composites are the most studied class of its kind, partly because of their application in the fabrication of mesoporous silica materials.[1d] Different from some other SI composites, the polymerization of silicate species along with the coassembly process further hardens the silicate−surfactant composites.[1] As a result, external driving forces are needed to destabilize the composites. A strong alkaline condition or a HF solution can disassemble the composites by etching the silica moiety, but it usually proceeds too fast to control. Under neutral or generic acidic conditions, however, the etching of silica proceeds rather slowly. Recently, it was found that the controlled dissolution of silica can be performed under neutral or acidic media, at a relatively higher temperature.[10−12] In this work, we developed a simple method for the rational disassembly of a SiO_2/CTAB mesophase ($mSiO_2$/CTAB) at room temperature. No alkaline agents were needed. The $mSiO_2$/CTAB composite was obtained from an alkaline synthesis, and the silicate−surfactant interaction was a S^+I^- Coulomb interaction (S^+ = surfactant cations; I^- = inorganic precursor anions).[1d,2a,3] One advantage of this method is that it can be used to selectively etch the silica framework within the composite mesophase over phase-pure silica. Interestingly, the partial disassembly of $mSiO_2$/CTAB spheres generally leads to the ready formation of hollow structures, which can be used for the synthesis of hollow mesoporous silica spheres (HMSs). This is a self-templating method that has been recently developed for the synthesis of hollow silica structures.[10−16]

EXPERIMENTAL SECTION

Materials. Tetraethyl orthosilicate (TEOS; A.R.), cetyltrimethylammonium bromide (CTAB; A.R.), $KMnO_4$ (A.R.), $K_3Fe(CN)_6$, poly(vinylpyrrolidone) (PVP) K30 (M_w ∼ 30000), ammonium hydroxide (28%), hydrochloric acid (36−38%), H_2O_2 (30%), sulfuric acid (98%), and absolute ethanol were purchased from Beijing Chemical Regent Company. Deionized water was used for all of the syntheses.

Preparation of $mSiO_2$/CTAB Spheres. A total of 1.2 g of CTAB was dissolved in a mixture of 40 mL of ethanol and 60 mL of water. Then into the surfactant solution were added 0.8 mL of an ammonia solution and 1.6 mL of TEOS in sequence. The reaction mixture was stirred for 10 h. Then the $mSiO_2$/CTAB spheres were isolated by centrifugation and washed with ethanol at least three times.

Preparation of Stöber Silica Spheres. The preparation of silica spheres involves the ammonia-catalyzed hydrolysis and condensation of TEOS in an aqueous ethanol solution via the classical Stöber method.[17] Typically, 45 mL of absolute ethanol, 15 mL of water, and 2 mL of a 28% ammonia solution were mixed and stirred. A total of 3.6 mL of TEOS was added into the mixture quickly. After a reaction time of about 10 h, the silica spheres were isolated by centrifugation. Then the white precipitate was washed with ethanol three times.

Preparation of HMSs from $mSiO_2$/CTAB Spheres. A total of 0.04 g of $mSiO_2$/CTAB spheres was dispersed into 15 mL of water via sonication. A total of 0.02 g of $KMnO_4$ or 0.1 g of $K_3Fe(CN)_6$ was dissolved in 5 mL of water. Then the salt solution was added into the $mSiO_2$/CTAB dispersion under stirring. After about 12 h, the product was isolated by centrifugation and washed with water. The precipitate

Received: June 27, 2012
Published: August 16, 2012

   dx.doi.org/10.1021/ic301371q | Inorg. Chem. 2012, 51, 9539−9543

was then treated with a HCl/H_2O_2 solution to remove the manganese species. In the case of $K_3Fe(CN)_6$, the precipitate was washed with ethanol several times to remove the iron impurity adsorbed. For surface-protected etching, the $mSiO_2$/CTAB spheres were pretreated with a PVP aqueous solution (0.16 g, 25 mL) for 24 h. Then the PVP-capped $mSiO_2$/CTAB spheres were isolated and treated with $KMnO_4$ or $K_3Fe(CN)_6$. Finally, the products were dried at 100 °C and calcined at 550 °C for 6 h to remove CTAB.

Preparation and Etching of $sSiO_2$@$mSiO_2$/CTAB and $mSiO_2$/CTAB@$sSiO_2$ Core–Shell Spheres. For the preparation of $sSiO_2$@$mSiO_2$/CTAB spheres, 0.02 g of $sSiO_2$ spheres was dispersed into 15 mL of water by soaking and sonication. Then 10 mL of ethanol and 0.1 g of CTAB were dissolved in the dispersion, followed by the addition of 0.2 mL of an ammonia solution and 0.1 mL of TEOS. The mixture was stirred for 10 h. The product was isolated and washed with ethanol three times. The sample was etched with $KMnO_4$ as described above. Surface-protected etching experiments were also carried out.

For the preparation of $mSiO_2$/CTAB@$sSiO_2$ spheres, 0.03 g of $mSiO_2$/CTAB spheres was dispersed into 5 mL of water and 15 mL of ethanol. Then 0.2 mL of an ammonia solution and 0.1 mL of TEOS were added, and the mixture was stirred for 10 h. After isolation and washing, the particles were dispersed into water and etched with a $KMnO_4$ solution as described above. The impurities were removed with a HCl/H_2O_2 solution, and the obtained particles can be used for another cycle of etching.

Characterizations. The morphology and structure of the silica particles were determined by a Hitachi H-7500 transmission electron microscope (TEM) operating at 80 kV and a Tecnai G2 F20 S-Twin high-resolution transmission electron microscope operating at 200 kV. Scanning electron microscopy (SEM) images were obtained on a FEI Sirion 200 field-emission microscope. The X-ray diffraction (XRD) patterns were collected by a Rigaku D/max-2500/PC X-ray diffractometer using Cu Kα radiation (λ = 1.5481 Å). The N_2 adsorption experiments were carried out on a Micromeritics Tristar II 3020 system at 77 K. The samples were pretreated at 473 K for 2 h under N_2 before measurements. The pore-size distributions were calculated from desorption branches of isotherms by the Barrett–Joyner–Halenda method. Elemental analysis was carried out by inductively coupled plasma optical emission spectroscopy technique using a 2RIS Intrepid II XSP inductively coupled plasma optical emission spectrometer.

RESULTS AND DISCUSSION

Typically, the disassembly of $mSiO_2$/CTAB was carried out in two steps. First, an aqueous dispersion of $mSiO_2$/CTAB spheres was stirred with a $KMnO_4$ aqueous solution overnight. Then the obtained solid product was further treated with a HCl/H_2O_2 mixture to remove the manganese impurities. As demonstrated in Figure 1a,b, the $mSiO_2$/CTAB spheres were preferentially dissolved in the interior after $KMnO_4$ treatment, resulting in hollow spheres. The impurities around the spheres in Figure 1b are believed to originate from the redox reactions between $KMnO_4$ and the surface-bound ethoxy groups.[18] All of the manganese species can be removed from the sample by reducing them into soluble Mn^{2+} in HCl/H_2O_2. The obtained hollow $mSiO_2$/CTAB spheres can be transformed into HMSs after surfactant removal (Figure 1c,d).

If the present method is carried out using PVP-capped $mSiO_2$/CTAB spheres as the starting material, the disassembly of the $mSiO_2$/CTAB spheres proceeds in a very different way. As illustrated in Figure 2a, dissolution of the PVP-capped spheres mainly occurred between the core and shell, resulting in rattle-type HMSs. The result of SEM observation shows that this surface-protected disassembly will generate additional openings in the silica shells (Figure 2b), which is quite different from the unprotected way (Figure 1d). A close

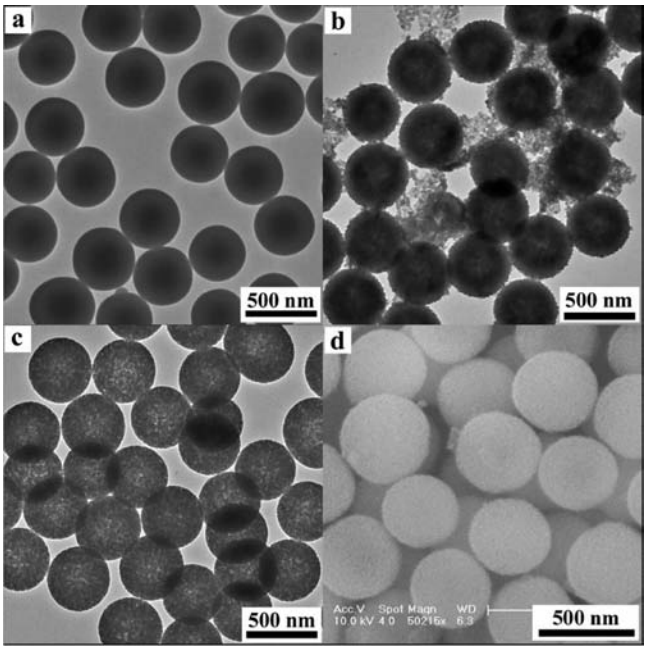

Figure 1. Transmission electron microscopy (TEM) micrographs of the precursor $mSiO_2$/CTAB spheres (a), the corresponding product after treatment with $KMnO_4$ (b), and the final HMSs after further removal of the manganese species and the surfactant template (c). (d) SEM image of the HMSs.

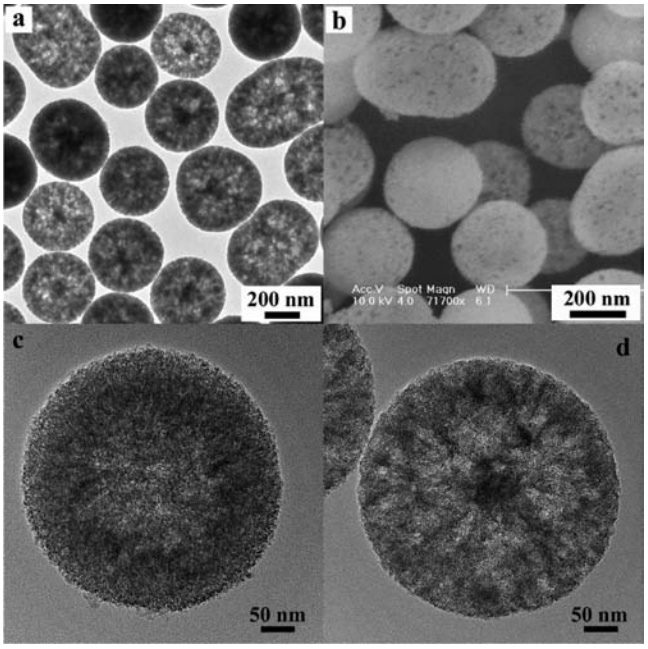

Figure 2. TEM (a) and SEM (b) images of rattle-type silica HMSs prepared with PVP-capped $mSiO_2$/CTAB and typical HRTEM images of normal (c) and rattle-type (d) hollow spheres.

observation of the two kinds of HMSs under high-resolution TEM (HRTEM) also proves this difference (Figure 2c,d). For convenience, the normal and rattle-type HMS samples are denoted as HMS-1 and HMS-2, respectively.

We characterize the pore structures of the two kinds of HMSs with the N_2 adsorption–desorption and XRD measurements. Figure 3 shows the N_2 adsorption–desorption isotherms and corresponding pore-size distributions for

dx.doi.org/10.1021/ic301371q | Inorg. Chem. 2012, 51, 9539–9543

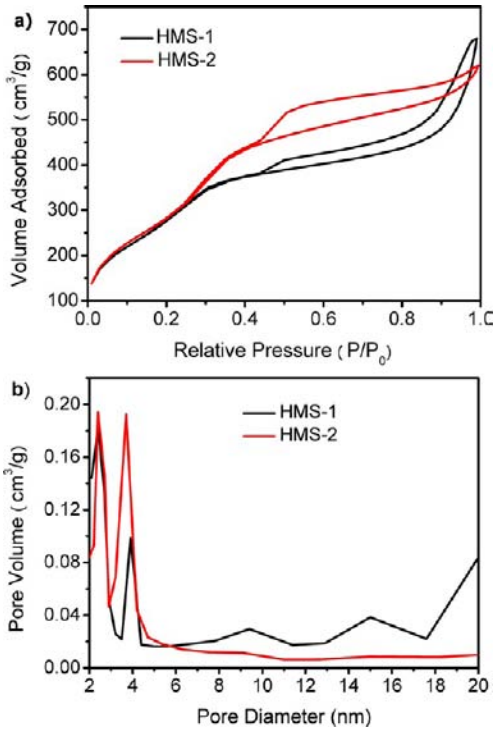

Figure 3. N_2 adsorption−desorption isotherms (a) and the corresponding pore-size distributions (b) of HMS-1 and HMS-2.

HMS-1 and HMS-2. HMS-1 and HMS-2 showed type IV N_2 adsorption isotherms,[19] and the measured specific surface areas were 1020 and 1045 $m^2\ g^{-1}$, respectively. Interestingly, both samples exhibit an obviously bimodal pore-size distribution in the range of 2−5 nm. As illustrated in Figure 3b, HMS-1 and HMS-2 have small pore fractions both centered at 2.4 nm, accompanied by relatively larger pore fractions centered at 3.9 and 3.7 nm, respectively. The smaller pores (2.4 nm) of the two samples are believed to be from the silica framework of the precursor spheres (Figure S1 in the Supporting Information, SI), which are only slightly affected during the disassembly process. The other wider pores might be due to etching of the silica wall by $KMnO_4$. The small-angle XRD patterns of HMS-1 and HMS-2 exhibit obvious left shifts relative to the precursor spheres (Figure S2 in the SI), indicative of enlarged average unit cell parameters upon $KMnO_4$ treatment.

The present disassembly of $mSiO_2$/CTAB spheres is not based on the alkaline etching of the silica wall because the $KMnO_4$ aqueous solution is almost neutral. Here, we propose an anion-exchange mechanism to explain the disassembly of the SiO_2/CTAB composite mesophase. In an aqueous dispersion of $mSiO_2$/CTAB spheres, positive charges of the CTAB micelles and negative charges of the silica wall are distributed according to the charge-density matching requirement.[20] Dissolution of the silica wall into bulk water was quite limited because of the slow dissolution kinetics of silica and the restriction of the surfactant micelles. In the present condition, permanganate ions have strong binding interaction to the surfactant moieties in the spheres, which reduced the silicate−surfactant interaction and thus accelerated the dissolution of silica into bulk water. The exchange between permanganate and silicate ions can be illustrated by eqs 1 and 2:

$$mSiO_2/CTAB(s) \rightleftharpoons \text{silicate} - CTAB(\text{complex}) \quad (1)$$

$$\text{silicate} - CTAB(\text{complex}) + MnO_4^-(aq) \rightleftharpoons MnO_4^- - CTAB(\text{complex}) + \text{silicate}(aq) \quad (2)$$

However, spontaneous formation of the hollow structure of HMS-1 is elusive. We estimate that this anion exchange emerges as the interdiffusion of permanganate and the dissolved silicate. The outward diffusion of silicate ions results in hollowed-out $mSiO_2$/CTAB spheres. Elemental analysis also supports the decrease of manganese and the emergence of appreciable amounts of silicon in the bulk solution after reaction (Figure S3 and Table S1 in the SI). All of the manganese impurities (within and around the hollow spheres) can be removed by reducing them into soluble manganese(II) ions in an acidic H_2O_2 solution. The proposed mechanism was illustrated in Figure 4a,b(1). As-made hollow $mSiO_2$/CTAB spheres can be further disassembled in another cycle of anion exchange (see below).

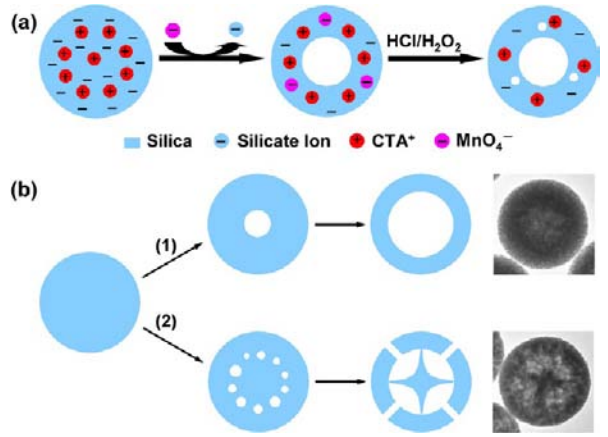

Figure 4. (a) Schematic illustration of the anion-exchange-driven disassembly of $mSiO_2$/CTAB spheres. (b) Typical structures and proposed formation routes for HMS-1 (1) and HMS-2 (2).

In the synthesis of HMS-2, PVP molecules on the $mSiO_2$/CTAB surface may have two functions: (1) protecting the silica surface from oxidation and dissolution,[13] which is evidenced by the largely reduced amount of the manganese impurities around the spheres (Figure S4 in the SI), and (2) serving as physical barriers, slowing down the mass-transfer rate at the solid−liquid interface and the interdiffusion within the sphere. We estimate that the formation process of HMS-2 is as follows: The presence of the PVP molecules blocks the normal outward diffusion of the silicate. The silica wall begins to dissolve between the core and shell parts, leaving many small voids. Then the etching of the silica wall can also proceed via a surface diffusion mode, giving rise to coalescence of the voids and the formation of obvious openings to release the dissolved silicate, as demonstrated in Figure 4b(2). The mechanism proposed here refers to the surface diffusion mechanism in Kirkendall diffusion systems.[21]

A nonacidic medium and the presence of the surfactant moiety in the $mSiO_2$/CTAB spheres are necessary for the present disassembly method. As illustrated in Figure 5a, no appreciable disassembly of the $mSiO_2$/CTAB spheres was observed in an acidic $KMnO_4$ solution. This is because an acidic medium will suppress dissolution of the silica wall. The presence of the surfactant moiety in the $mSiO_2$/CTAB spheres is crucial to the anion-exchange-driven process illustrated in eqs

dx.doi.org/10.1021/ic301371q | Inorg. Chem. 2012, 51, 9539−9543

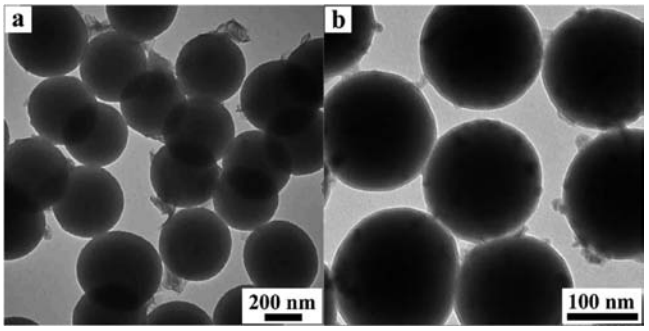

Figure 5. (a) TEM images of $mSiO_2$/CTAB spheres treated with an acidic $KMnO_4$ solution (in sulfuric acid, pH ~1.8). (b) Stöber silica spheres treated with a $KMnO_4$ solution.

1 and 2. Therefore, Stöber silica spheres, which contain no cationic surfactant moieties, cannot be used to synthesize hollow silica spheres using the present method. As a matter of fact, they can hardly be affected by $KMnO_4$ treatment except that some redox reaction may occur on the silica surface (Figure 5b). Moreover, the kind of surfactant also has great effect on the present disassembly method; mesophases using surfactants other than CTAB might also be disassembled to some extent, but not necessarily giving hollow structures (Figure S5 in the SI).

We further proved the selective etching of $mSiO_2$/CTAB over solid silica ($sSiO_2$) using the following experiments. Two core–shell structured samples, $sSiO_2$@$mSiO_2$/CTAB and $mSiO_2$/CTAB@$sSiO_2$, were etched with the standard two-step disassembly method. The results were given in Figure 6a–f. For the $sSiO_2$@$mSiO_2$/CTAB spheres, the surrounding $mSiO_2$/CTAB shells became much less dense after $KMnO_4$ treatment, while the $sSiO_2$ cores remained almost unchanged (Figure 6a–c). The surface protection effect was also obvious for PVP-capped $sSiO_2$@$mSiO_2$/CTAB spheres (Figure 6c). For $mSiO_2$/CTAB@$sSiO_2$ (the $sSiO_2$ shell is very thin relative to the core, ;Figure 6d), we carried out two cycles of etching (see the Experimental Section). After the first cycle of etching, the cores became less dense (Figure 6e). After the second cycle of etching, the $mSiO_2$/CTAB cores were largely dissolved; the thin silica shells could not support themselves and collapsed, like deflated balloons (Figure 6f). Several reports have shown the selective etching of $sSiO_2$ over $mSiO_2$/CTAB.[16,22] However, the reverse case was not reported as far as we know. Herein, it is simply realized by using the anion-exchange-driven etching method. It is expected that our methods may be useful in the fabrication of some complex silica-based structures.

In this work, $KMnO_4$ as an etching agent was chosen fortuitously, in spite of its effectiveness. It seems that other $KMnO_4$-like regents can also be used in the fabrication of HMSs by the anion-exchange disassembly method. Indeed, we found that another regent, $K_3Fe(CN)_6$, performed similarly to $KMnO_4$ (Figures 6g–i and S6 in the SI). However, some other regents, such as $K_2Cr_2O_7$ and Na_2MoO_4, worked not as well (Figure S7 in the SI). The reason is not very clear at the moment.

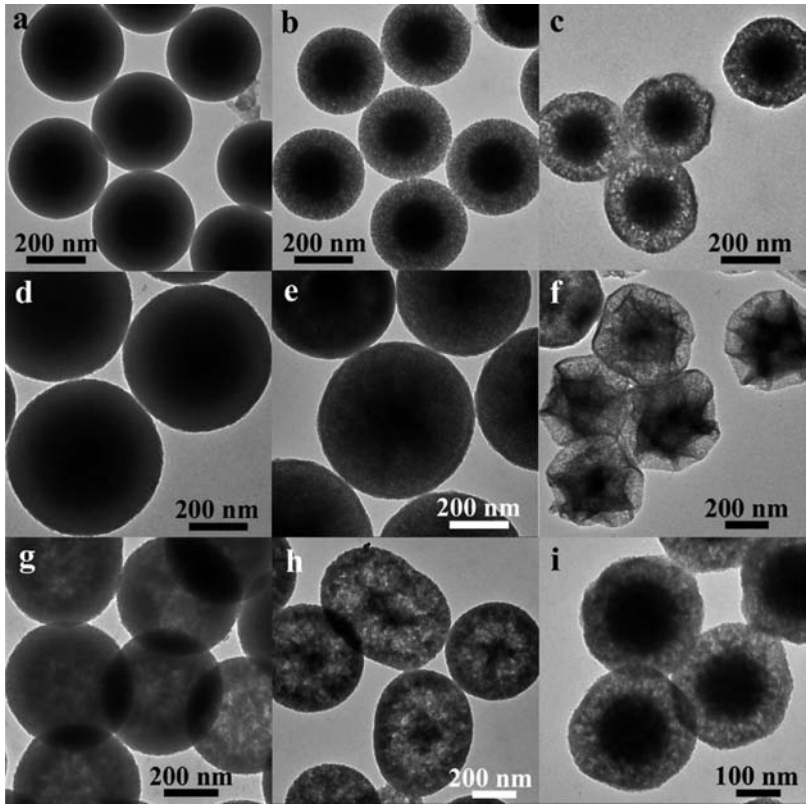

Figure 6. TEM images of $sSiO_2$@$mSiO_2$/CTAB spheres (a) and corresponding products obtained by the present method under the normal way (b) and under the surface-protected way (c). TEM images of $mSiO_2$/CTAB@$sSiO_2$ spheres (d) and corresponding products obtained by etching them with the present method once (e) and twice (f). TEM images of products obtained by etching $mSiO_2$/CTAB (g), PVP-capped $mSiO_2$/CTAB (h), and $sSiO_2$@$mSiO_2$/CTAB spheres (i) with $K_3Fe(CN)_6$.

dx.doi.org/10.1021/ic301371q | Inorg. Chem. 2012, 51, 9539–9543

CONCLUSION

In conclusion, we developed an advanced method to disassemble a SiO_2/CTAB composite mesophase in a neutral medium at room temperature. Using $KMnO_4$ as a typical etching agent, hollow/rattle-type mesoporous silica spheres were prepared by the partial disassembly of SiO_2/CTAB mesophase spheres. The disassembly process was supposed to be driven by anion exchange between permanganate and silicate ions. Significantly, the present method realized the highly selective etching of mesophase SiO_2/CTAB over the silica phase and thus may be utilized to fabricate some complex silica-based structures. This mild method may be extended to the disassembly of other SI composite materials and might be interesting in demineralization.

ASSOCIATED CONTENT

Supporting Information

Additional TEM images, XRD patterns, and N_2 adsorption results corresponding to the disassembly of a SiO_2/CTAB mesophase. This material is available free of charge via the Internet at http://pubs.acs.org.

AUTHOR INFORMATION

Corresponding Author

*E-mail: wangxun@mail.tsinghua.edu.cn.

Notes

The authors declare no competing financial interest.

ACKNOWLEDGMENTS

This work was supported by the NSFC (Grants 91127040 and 20921001), the State Key Project of Fundamental Research for Nanoscience and Nanotechnology (Grant 2011CB932402), and the China Postdoctoral Science Foundation (Grant 2011M500283).

REFERENCES

(1) (a) Firouzi, A.; Kumar, D.; Bull, L. M.; Besier, T.; Sieger, P.; Huo, Q.; Walker, S. A.; Zasadzinski, J. A.; Glinka, C.; Nicol, J.; Margolese, D.; Stucky, G. D.; Chmelka, B. F. *Science* **1995**, *267*, 1138−1143. (b) Sellinger, A.; Weiss, P. M.; Nguyen, A.; Lu, Y.; Assink, R. A.; Gong, W.; Brinker, C. J. *Nature* **1998**, *394*, 256−260. (c) Tanev, P. T.; Pinnavaia, T. J. *Science* **1996**, *271*, 1267−1269. (d) Wan, Y.; Zhao, D. Y. *Chem. Rev.* **2007**, *107*, 2821−2860.

(2) (a) Huo, Q.; Margolese, D. I.; Ciesla, U.; Feng, P.; Gier, T. E.; Sieger, P.; Leon, R.; Petroff, P. M.; Schüth, F.; Stucky, G. D. *Nature* **1994**, *368*, 317−321. (b) Yang, P.; Zhao, D.; Margolese, D. I.; Chmelka, B. F.; Stucky, G. D. *Nature* **1998**, *396*, 152−155.

(3) Huo, Q. S.; Margolese, D. I.; Ciesla, U.; Demuth, D. G.; Feng, P. Y.; Gier, T. E.; Sieger, P.; Firouzi, A.; Chmelka, B. F.; Schuth, F.; Stucky, G. D. *Chem. Mater.* **1994**, *6*, 1176−1191.

(4) (a) Li, H. L.; Sun, H.; Qi, W.; Xu, M.; Wu, L. X. *Angew. Chem., Int. Ed.* **2007**, *46*, 1300−1303. (b) Nisar, A.; Zhuang, J.; Wang, X. *Chem. Mater.* **2009**, *21*, 3745−3751. (c) Nisar, A.; Lu, Y.; Wang, X. *Chem. Mater.* **2010**, *22*, 3511−3518.

(5) (a) Trikalitis, P. N.; Rangan, K. K.; Bakas, T.; Kanatzidis, M. G. *Nature* **2001**, *410*, 671−675. (b) Trikalitis, P. N.; Rangan, K. K.; Bakas, T.; Kanatzidis, M. G. *J. Am. Chem. Soc.* **2002**, *124*, 12255−12260. (c) Xu, B.; Wang, R. J.; Wang, X. *Nanoscale* **2012**, *4*, 2713−2719.

(6) Kim, Y.-Y.; et al. *Nat. Mater.* **2011**, *10*, 890−896.

(7) Mizutani, M.; Yamada, Y.; Yano, K. *Chem. Commun.* **2007**, 1172−1174.

(8) Mizutani, M.; Yamada, Y.; Nakamura, T.; Yano, K. *Chem. Mater.* **2008**, *20*, 4777−4782.

(9) Liu, M.-C.; Sheu, H.-S.; Cheng, S. *J. Am. Chem. Soc.* **2009**, *131*, 3998−4005.

(10) Hu, Y. X.; Zhang, Q.; Geobl, J.; Zhang, T. R.; Yin, Y. D. *Phys. Chem. Chem. Phys.* **2010**, *12*, 11836−11842.

(11) Yu, Q. Y.; Wang, P. P.; Hu, S.; Hui, J. F.; Zhuang, J.; Wang, X. *Langmuir* **2011**, *27*, 7185−7191.

(12) Wong, Y. J.; Zhu, L.; Teo, W. S.; Tan, Y. W.; Yang, Y.; Chen, H. *J. Am. Chem. Soc.* **2011**, *133*, 11422−11425.

(13) (a) Zhang, Q.; Zhang, T. R.; Ge, J. P.; Yin, Y. D. *Nano Lett.* **2008**, *8*, 2867−2871. (b) Zhang, Q.; Ge, J. P.; Goebl, J.; Hu, Y. X.; Lu, Z. D.; Yin, Y. D. *Nano Res.* **2009**, *2*, 583−591.

(14) (a) Zhang, T. R.; Ge, J. P.; Hu, Y. X.; Zhang, Q.; Aloni, S.; Yin, Y. D. *Angew. Chem., Int. Ed.* **2008**, *47*, 5806−5811. (b) Zhang, T. R.; Zhang, Q.; Ge, J. P.; Goebl, J.; Sun, M. W.; Yan, Y. S.; Liu, Y. S.; Chang, C. L.; Guo, J. H.; Yin, Y. D. *J. Phys. Chem. C* **2009**, *113*, 3168−3175.

(15) Zhang, Q.; Wang, W. S.; Goebl, J.; Yin, Y. D. *Nano Today* **2009**, *4*, 494−507.

(16) Fang, X. L.; Chen, C.; Liu, Z. H.; Liu, P. X.; Zheng, N. F. *Nanoscale* **2011**, *3*, 1632−1639.

(17) Stöber, W.; Fink, A.; Bohn, E. *J. Colloid Interface Sci.* **1968**, *26*, 62−69.

(18) Costa, C. A. R.; Leite, C. A. P.; Galembeck, F. *J. Phys. Chem. B* **2003**, *107*, 4747−4755.

(19) IUPAC reporting physisorption data for gas/solid system: *Pure Appl. Chem.* **1985**, *57*, 603−619.

(20) Monnier, A.; Schüth, F.; Huo, Q.; Kumar, D.; Margolese, D.; Maxwell, R. S.; Stucky, G. D.; Krishnamurty, M.; Petroff, P.; Firouzi, A.; Janicle, M.; Chmelka, B. F. *Science* **1993**, *261*, 1299−1303.

(21) (a) Fan, H. J.; Knez, M.; Scholz, R.; Hesse, D.; Nielsch, K.; Zacharias, M.; Gösele, U. *Nano Lett.* **2007**, *7*, 993−997. (b) Fan, H. J.; Gösele, U.; Zacharias, M. *Small* **2007**, *3*, 1660−1671.

(22) (a) Chen, Y.; Chen, H. R.; Guo, L. M.; He, Q. J.; Chen, F.; Zhou, J.; Feng, J. W.; Shi, J. L. *ACS Nano* **2010**, *4*, 529−539. (b) Chen, Y.; Chen, H. R.; Ma, M.; Chen, F.; Guo, L. M.; Zhang, L. X.; Shi, J. L. *J. Mater. Chem.* **2011**, *21*, 5290−5298.